5036–5044 *Nucleic Acids Research, 1998, Vol. 26, No. 22*

The c-*myc* coding region determinant-binding protein: a member of a family of KH domain RNA-binding proteins

Glenn A. R. Doyle, Natalie A. Betz[1], Peter F. Leeds, Ani J. Fleisig, Rebecca D. Prokipcak[2] and Jeff Ross*

McArdle Laboratory for Cancer Research, University of Wisconsin-Madison, 1400 University Avenue, Madison, WI 53706, USA, [1]Promega Corporation, 2800 Woods Hollow Road, Madison, WI 53711-5399, USA and [2]Department of Pharmacology, Room 4308 Medical Sciences Building, 8 Taddle Creek Road, University of Toronto, Toronto, Ontario M5S 1A8, Canada

Received September 11, 1998; Accepted September 28, 1998

DDBJ/EMBL/GenBank accession no. AF061569

ABSTRACT

The half-life of c-*myc* mRNA is regulated when cells change their growth rates or differentiate. Two regions within c-*myc* mRNA determine its short half-life. One is in the 3′-untranslated region, the other is in the coding region. A cytoplasmic protein, the coding region determinant-binding protein (CRD-BP), binds *in vitro* to the c-*myc* coding region instability determinant. We have proposed that the CRD-BP, when bound to the mRNA, shields the mRNA from endonucleolytic attack and thereby prolongs the mRNA half-life. Here we report the cloning and further characterization of the mouse CRD-BP, a 577 amino acid protein containing four hnRNP K-homology domains, two RNP domains, an RGG RNA-binding domain and nuclear import and export signals. The CRD-BP is closely related to the chicken β-actin zipcode-binding protein and is similar to three other proteins, one of which is overexpressed in some human cancers. Recombinant mouse CRD-BP binds specifically to c-*myc* CRD RNA *in vitro* and reacts with antibody against human CRD-BP. Most of the CRD-BP in the cell is cytoplasmic and co-sediments with ribosomal subunits.

INTRODUCTION

The c-Myc protein is a helix–loop–helix/leucine zipper (HLH/LZ) type transcription factor that forms heterodimers with Max (1–3). c-Myc abundance influences cell proliferation, differentiation and neoplastic transformation (4–7) and c-Myc overexpression is implicated in tumor formation (8,9). These and other consequences of aberrant c-*myc* expression highlight the importance of understanding c-*myc* gene regulation.

c-Myc protein expression is regulated at multiple levels and is strongly influenced by changes in c-*myc* mRNA stability (10–12). The half-life of c-*myc* mRNA is usually 15–30 min but can be 2 h or more in some cells under some conditions. For example, the c-*myc* gene is active and c-*myc* mRNA is relatively stable in fetal rodent hepatocytes. As a result, fetal hepatocytes contain abundant c-*myc* mRNA. The c-*myc* gene is also active in adult hepatocyes, but the mRNA is quite unstable. As a result, adult hepatocytes contain little or no c-*myc* mRNA (13,14). The mRNA is transiently up-regulated and stabilized in adult hepatocytes following partial hepatectomy (15,16). These findings illustrate how c-*myc* mRNA stability affects c-MYC protein expression.

Two *cis*-acting sequence elements affect the post-transcriptional regulation of c-*myc* mRNA: an AU-rich element (AURE) in the 3′-untranslated region (3′-UTR) and an ~250 nt coding region instability determinant (CRD). The CRD encodes part of the HLH/LZ domain and is located at the 3′-terminus of the coding region. Four observations show that this CRD functions independently of the AURE to affect c-*myc* mRNA expression: (i) c-*myc* mRNA lacking its CRD is more stable than wild-type c-*myc* mRNA (17–20); (ii) the CRD is required for the post-transcriptional down-regulation of c-*myc* mRNA that occurs when cultured myoblasts fuse to form myotubes (20,21); (iii) the c-*myc* CRD functions as an mRNA-destabilizing element when fused in-frame within the coding region of β-globin mRNA (22); (iv) the c-*myc* CRD is required for up- and down-regulating c-*myc* mRNA abundance post-transcriptionally in transgenic mice undergoing liver regeneration following partial hepatectomy (13,15,16,23–25).

We have investigated how the CRD affects c-*myc* expression using a cell-free mRNA decay system that includes polysomes from cultured cells. The polysomes contain both the substrates (mRNAs) for decay and at least some of the enzymes and co-factors that affect mRNA stability. Polysomes are incubated in an appropriate buffer and the decay rates of endogenous polysomal mRNAs such as c-*myc* are monitored by hybridization. This *in vitro* assay reflects many aspects of mRNA decay in intact cells (26–29). For example, mRNAs that are unstable in cells are also unstable *in vitro*, while mRNAs that are stable in cells are stable *in vitro* (26). In standard reactions, polysome-associated c-*myc* mRNA is degraded rapidly in a 3′→5′ direction, perhaps by an exonuclease (29). An alternative endonucleolytic decay pathway is activated when the reactions are supplemented with a 180 nt sense strand competitor RNA corresponding to part of the c-*myc* CRD. This RNA induces endonucleolytic cleavage within the c-*myc* CRD, thereby destabilizing c-*myc* mRNA 8-fold (30). This effect is highly specific. Other competitor RNAs do not destabilize c-*myc* mRNA and c-*myc* CRD competitor RNA does not destabilize other mRNAs tested.

*To whom correspondence should be addressed. Tel: +1 608 262 3413; Fax: +1 608 262 9464; Email: ross@oncology.wisc.edu

Based on these observations, we suggested the following model: (i) the c-*myc* CRD is susceptible to attack by a ribosome-associated endoribonuclease; (ii) a protein can bind to the CRD and shield the CRD from the RNase; (iii) *in vitro*, when we add competitor CRD RNA to the reactions, the competitor titrates the protein off c-*myc* mRNA, leaving the CRD unprotected and open to attack by the RNase. Consistent with this model, we detected a protein that binds *in vitro* to c-*myc* CRD [^{32}P]RNA (30). This protein, the c-*myc* coding region determinant-binding protein (CRD-BP), was purified to homogeneity (31). We then found that the CRD-BP is developmentally regulated, being expressed in fetal and neonatal rats but not in adult animals (32).

Here we report the cloning of full-length mouse and partial human CRD-BP cDNAs. CRD-BP derived from the mouse cDNA exhibits RNA-binding properties identical to those of CRD-BP purified from cells. The CRD-BP is primarily a cytoplasmic protein that co-sediments with polysomes. These observations are consistent with a role for the CRD-BP in shielding polysomal c-*myc* mRNA from endonucleolytic attack. The CRD-BP is a member of a family of RNA-binding proteins containing four KH regions.

MATERIALS AND METHODS

Cell lines and preparation of subcellular fractions

Cell lines were obtained from the American Type Culture Collection (Rockville, MD). K562 human erythroleukemia cells were cultured as described (26). NIH 3T3, H4IIE and 293 cells were cultured in DMEM (4.5 g/l glucose) containing 10% calf serum and antibiotics (Gibco BRL). Polysomes and post-polysomal supernatant (S130) were prepared as described (26,30,31), but the cells were lysed in buffer A (1 mM potassium acetate, 1.5 mM magnesium acetate, 2 mM DTT, 10 mM Tris–HCl, pH 7.4) supplemented with 0.1 mM EGTA, 100 µg/ml PMSF and 2 µg/ml each of aprotinin, leupeptin and pepstatin A (Sigma). The nuclear pellet from the first low speed centrifugation was washed once in buffer A and centrifuged. Nuclear wash material in the supernatant was harvested and saved. The nuclei were then resuspended in 300 µl of buffer B (1.5 mM $MgCl_2$, 140 mM NaCl, 20% v/v glycerol, 10 mM Tris–HCl, pH 8.0), lysed by adding 2.7 ml of buffer C (5.0% w/v SDS, 10% v/v glycerol, 5% v/v β-mercaptoethanol, 62.5 mM Tris–HCl, pH 6.8), passed 10 times through an 18 gauge needle and boiled for 15 min. Ribosomal salt washes (RSW) from cells and from translation reactions were prepared as described (31). All fractions were stored at –70°C.

Protein purification and microsequencing

Two independent preparations of human c-*myc* CRD-BP were purified from K562 cell RSW (31). One was microsequenced at the Protein Sequence and Peptide Synthesis Facility of the University of Wisconsin Biotechnology Center (Madison, WI), the other at the Keck Laboratories, Yale University (New Haven, CT). This second sequence was distinct from the first, did not overlap and was used to design PCR primers.

Cloning of CRD-BP cDNAs

Human CRD-BP cDNA cloning. We first prepared a human CRD-BP cDNA and used it to identify mouse CRD-BP cDNA. A K562 (human) cell cDNA λ library (Clontech) was screened by degenerate PCR to amplify a 45 bp DNA sequence based on the 15 amino acids of the second CRD-BP peptide sequence. The primers were: 5′-GTBAAYGARYTBCARAA-3′ (coding) and 5′-GGVACVACVACYTCDGC-3′ (non-coding). A 45 bp product encoding the expected 15 amino acid sequence was isolated. A combination of non-degenerate PCR and library screening generated a 1069 bp partial human CRD-BP cDNA with an open reading frame (ORF) encoding both sequenced peptides. Additional segments of the human cDNA were cloned via 3′ rapid amplification of cDNA ends (3′-RACE). Oligomer Not(dT) (5′-AACCCGGCTCGAGCGGCCGCTTTTTTTTTTTTTTT-TT-3′) and Superscript II (Gibco BRL) were used to reverse transcribe 0.5 µg of K562 cell poly(A)$^+$ mRNA. The cDNA template was then amplified using oligomers CRD-BP1 (5′-ACGG-CAGCTGAGGTGGTAGTACC-3′) and NotAdaptmer (5′-AACC-CGGCTCGAGCGGCCGCT-3′) as 5′ and 3′ primers, respectively.

Mouse CRD-BP cDNA cloning. The partial human CRD-BP cDNA was used to identify two mouse CRD-BP cDNAs in the EST database. The larger one, AA073514, was obtained from Genome Systems and was sequenced. Its amino acid sequence was 99% identical to that of our human CRD-BP, indicating that it corresponded to mouse CRD-BP. It contained the entire 3′-UTR and most of the coding region. To extend the 5′ sequence, 5′-RACE was performed on a 17 day mouse embryo Marathon-Ready cDNA Library (Clontech). 'Touchdown PCR' was performed with oligomers AP1 (Clontech) and CRD-BP2 (5′-AGGTTCCGTC-CTTCCTTGCCAATG-3′) as 5′ and 3′ primers, respectively. Secondary PCR was then performed using nested 5′ and 3′ primers [AP2 (Clontech) and CRD-BP3 (5′-AACTTCATCTGCCGTTT-TGG-5′), respectively]. Since the resulting clone lacked the translation start site and 5′-UTR, a mouse BAC library (Genome Systems) was screened by PCR with primers CRD-BP4 (5′-CATC-AACTGGAGAACCATG-3′) and CRD-BP5 (5′-GACTGCGTC-TGTTTTGTGATG-3′). A BAC clone containing the mouse CRD-BP gene was obtained from Genome Systems. The remainder of the coding region and at least part of the 5′-UTR were sequenced from this BAC clone using CRD-BP6 (5′-CTGTAGGA-GATCTTGTGCTC-3′) as primer.

In vitro translation of mouse CRD-BP

The mouse CRD-BP cDNA ORF was subcloned via PCR into pSPUTK (Stratagene) to create the translation clone pSPUTK-CRD-BP. A single base mutation (underlined) in the 5′ primer (5′-CGCACCGCCACCATG<u>G</u>ACAAGCTTTACATCGG-3′) changed an asparagine to an aspartic acid at amino acid position 2. The 3′ primer (5′-ACTGGGATCTGACCCATCCT-3′) was from the CRD-BP 3′-UTR. To express mouse CRD-BP with a C-terminal 6-histidine (His_6) affinity tag, mouse CRD-BP was subloned into pET28b(+) (Novagen) cut with *Nco*I and *Xho*I. His_6–CRD-BP was purified from *Escherichia coli* using standard Ni^{2+}–agarose affinity chromatography (Qiagen). CRD-BP eluted from the column was dialyzed against 200 mM KCl, 1 mM EDTA, 10% (v/v) glycerol, 1 mM reduced glutathione, 0.1 mM oxidized glutathione, 20 mM triethanolamine, pH 7.6. cDNAs were transcribed and translated in the TnT® Coupled Reticulocyte Lysate System (Promega).

Immunoblotting and gel retardation assays

Immunoblotting for CRD-BP was performed using chicken anti-CRD-BP IgY against purified human protein (31,32). To detect heat shock protein 90 (HSP90), the primary antibody was

rabbit anti-mouse HSP90 polyclonal IgG (from Dr Alan Poland) and the secondary antibody was HRP-conjugated goat anti-rabbit IgG (Sigma). Reactive bands were visualized using enhanced chemiluminescence (ECL). Distinct bands were not detected with preimmune serum, normal human serum or secondary antibodies alone (data not shown). Where noted, blots were stripped for 30 min at 50°C in 2% SDS, 100 mM β-mercaptoethanol, 50 mM K_2HPO_4, pH 6.8, and were then washed extensively in buffer containing 5% non-fat dry milk. Gel retardation assays were performed as described (31,32). In competition assays, the CRD-BP was pre-incubated with or without unlabeled competitor RNA for 10 min at 30°C and then [^{32}P]RNA probe was added.

Sucrose gradient centrifugation and ribosomal RNA analysis

All procedures were performed at 4°C. A 50 µl aliquot of K562 cell polysomes was brought to 20 mM EDTA, mixed gently, left on ice for 20 min, layered over a 10 ml linear 5–30% sucrose gradient in buffer D (100 mM KCl, 10 mM potassium acetate, 5 mM EDTA, 1 mM DTT, 5 mM HEPES, pH 7.3; 34) and centrifuged in a Beckman SW41.1 rotor for 4 h at 38 000 r.p.m. (178 000 *g*). Fractions (500 µl) were pipetted sequentially from the top. Pelleted material was resuspended in 500 µl of buffer D containing 5% sucrose. Proteins were precipitated with methanol and chloroform prior to immunoblotting. RNA was isolated using TRIzol reagent (Gibco BRL), electrophoresed in a 1% agarose gel and visualized with ethidium bromide.

Transfections and immunofluorescence

To construct a mouse CRD-BP cDNA encoding an N-terminal FLAG tag, oligomers encoding the FLAG sequence (Top, 5′-CATGGACTACAAGGACGACGATGACAAGGT-3′; Bottom, 5′-CATGACCTTGTCATCGTCGTCCTTGTAGTC-3′) were kinased, annealed and ligated into *Nco*I-digested, dephosphorylated pSPUTK-CRD-BP to form pSPUTK-FLAG–CRD-BP. FLAG–CRD-BP and untagged CRD-BP cDNAs were then subcloned into pcDNA3 (Invitrogen) for mammalian expression. Each DNA was transfected by calcium phosphate precipitation into 293 or H4IIE cells grown on coverslips. Forty eight hours after transfection, cells were fixed in ice-cold methanol (H4IIE cells) or phosphate-buffered saline (PBS) containing 4% (v/v) formaldehyde (293 cells). Cells were then washed in PBS, permeabilized in PBS containing 0.1% (v/v) Triton X-100 and stained for FLAG–CRD-BP expression by immunofluorescence using anti-FLAG M2 monoclonal (Sigma) and FITC-conjugated goat anti-mouse IgG polyclonal (Sigma) as the secondary antibody (35). Fluorescently labeled cells were visualized under dark field optics at 63× magnification. Images were captured and digitized directly to a computer for storage and printing.

RESULTS

Cloning of CRD-BP cDNAs and identification of related genes

Two preparations of highly purified human CRD-BP were isolated and microsequenced. Each gave a different, non-overlapping sequence: P-A-Q-A-V-G-A-I-Q/I-G-k/r-I/K-Y/G-Q-X-i/l-k and V-N-E-L-Q-N-L-T-A-A-E-V-V-V-P (lower case letters indicate residues of less confidence than upper case letters). A 1069 bp

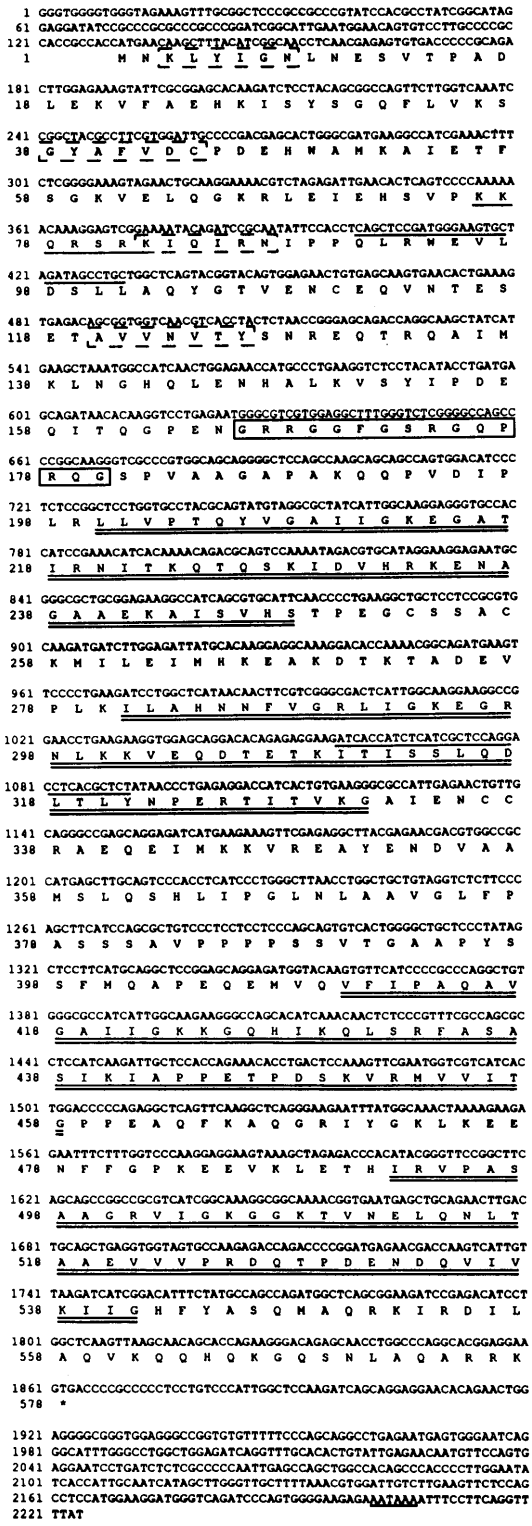

Figure 1. Mouse CRD-BP cDNA and predicted protein sequence. Sequences resembling nuclear localization and nuclear export signals, single underline and overlines, respectively. Sequences denoting the RGG box and KH domains, solid box and double underlines, respectively. The RNP1 and RNP2 sequences of each RRM, dashed boxes (Fig. 2). An asterisk indicates the translation termination site and the polyadenylation signal is single underlined. We have not demonstrated conclusively that the indicated translation start site is the correct or only start site. The 5′-UTR might be incomplete, since the transcription start site has not been mapped.

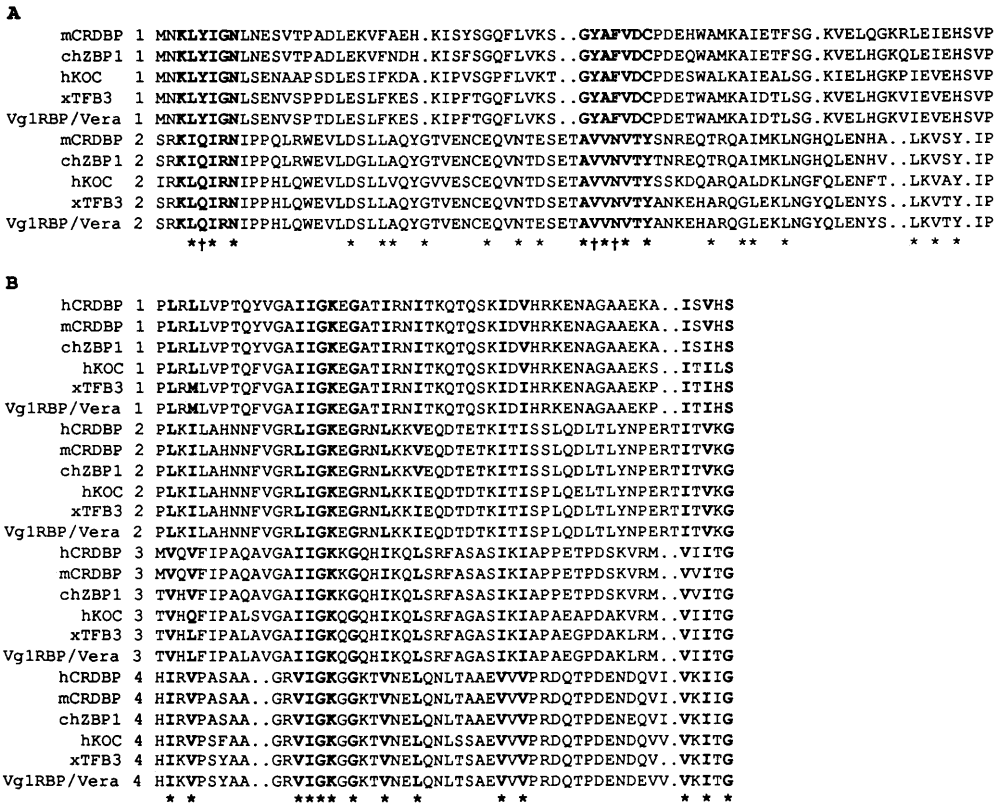

Figure 2. Alignments of RNA-binding domains of CRD-BP and related proteins. Human CRD-BP sequences are from EST AA196976. (**A**) RRM domains. The RNP-1 and RNP-2 domains of each RRM are in bold. Asterisks indicate conserved residues proposed to be important in forming the hydrophobic RRM core structure. Crosses (†) denote positions at which 'typical' RNP domains contain either Y or F (37 and references therein). hCRDBP RRM sequences are not shown, since this region is not present in the EST. (**B**) KH domains. KH domain consensus sequences (38) are shown in bold and by asterisks below the alignment. GenBank accession nos are as follows: mCRDBP, AF061569; hCRDBP EST, AA196976/AA196977; chZBP1, AF026527; hKOC, U97188; xTFB3, AF042353; Vg1 RBP/Vera, AF064633 and AF055923, respectively.

human cDNA was generated. It contained an ORF that included both peptide sequences obtained by microsequencing.

To continue our analysis of CRD-BP in rodents, we used human cDNA to isolate mouse CRD-BP cDNA, which contained at least a portion of the 5′-UTR, a complete coding region and a complete 3′-UTR (Fig. 1). Two in-frame AUG start codons are present near the 5′-terminus. We have tentatively designated the downstream AUG as the translation start site for two reasons: it is embedded within a preferred translation start signal (36) and is similar to the translation start of CRD-BP homologs (Fig. 2).

The predicted CRD-BP sequence includes three characteristic RNA-binding protein motifs (37): RNA recognition motifs (RRMs), an RGG box and four hnRNP K-homology (KH) domains. There are two RRMs in the N-terminal third of the protein (Fig 2A). The first RRM (dashed boxes in Fig. 1) contains typical RNP-1 and RNP-2 consensus sequences (38) as identified in ZBP1, the chicken β-actin zipcode-binding protein (accession no. AF026527; 33). The second putative RRM was not identified in ZBP1. Like the RRMs of polypyrimidine tract-binding protein (pPTB; accession no. X60648; 39) and hnRNP L (accession no. X16135; 40), the RNP sequences in this putative RRM diverge from the consensus sequences. Yet, the second RRM contains conserved hydrophobic residues thought to contribute to the RRM hydrophobic core (Fig. 2). Therefore, this region of the mouse CRD-BP fits the broader definition of an RRM. A putative RGG box that follows the RRMs (Fig. 1, boxed) is similar to RGG boxes in fibrillarin (accession no. X56597; 41), nucleolin (accession no. M60858; 42) and fragile-X mental retardation protein (FMRP; accession no. X69962; 43–45). Four KH domains are arranged in pairs (Fig. 1, double underlines). Each pair is separated by ~30 amino acids and the two pairs are separated by 78 amino acids. There are two putative nuclear export signals (NES, overlined) and a putative nuclear localization signal (NLS, underlined), which is also a feature of ZBP1 (33). One of the two NESs (ITISSLQDLTLY) is similar to that in HIV Rev protein (accession no. X58781; 46) and is located within the second KH domain. The second NES (QLRWEVLDSLL) is similar to one in FMRP (45).

In the rat, the CRD-BP is expressed abundantly during fetal development and neonatal life but is undetectable in adult tissues (32). It is also expressed in transformed tissue culture cell lines derived from adult organisms. These findings imply that the CRD-BP is an oncofetal protein. Consistent with this notion, all known CRD-BP Expressed Sequence Tags (ESTs) are derived from fetal or embryonic tissue (accession nos AA619650, AA399833, AA073173, AA073514, D76662, D76781, AA196976/AA196977 and AA196759/AA196774).

Table 1. Comparison of sequences of CRD-BP and related proteins

	hCRD-BP[a]	cZBP1	hKOC	xTFB3	xVg1 RBP/Vera
mCRD-BP	**88.8** 99.1 *99.3*	**82.5** 94.6 *95.7*	**69.5** 73.9 *79.1*	**71.0** 78.1 *84.1*	**70.2** 77.9 *83.8*
hCRD-BP		**82.0** 95.1 *96.0*	**69.5** 74.6 *78.6*	**69.5** 78.1 *83.5*	**70.4** 77.9 *83.9*
cZBP1			**70.0** 75.6 *80.1*	**72.0** 78.7 *84.5*	**72.2** 78.4 *84.1*
hKOC				**79.0** 84.1 *87.9*	**78.5** 83.4 *87.4*
xTFB3					**96.1** 97.6 *98.1*

Values in bold indicate nucleic acid sequence identity, plain type indicates protein sequence identity and italic indicates protein sequence similarity. Only coding sequences were analyzed.
[a]The human CRD-BP cDNA is a partial sequence.

Mouse and human CRD-BP are similar to four other proteins (Fig. 2 and Table 1): ZBP1; hKOC, which is overexpressed in human pancreatic cancer (accession no. U97188; 47); xTFB3, a transcription factor from *Xenopus* that binds the B3-element of the TFIIIA promoter (accession no. AF042353; 48); Vg1 RBP or Vera, which binds to the localization sequence in *Xenopus* Vg1 mRNA (accession nos AF064633 and AF055923; 49,50). Of this group, mouse and human CRD-BP are most homologous to chicken ZBP1 and clearly are not alternative forms of hKOC, xTFB3 or Vg1 RBP/Vera. The common motif organization and considerable homology among these proteins suggest that they constitute a new subfamily of RNA-binding proteins (see below).

Comparison of *in vitro* synthesized CRD-BP with cell-derived CRD-BP

To confirm that our murine cDNA clone encodes a c-*myc* mRNA-binding protein, we synthesized the protein *in vitro* and analyzed it by immunoblotting and gel retardation. Reticulocyte transcription/translation reactions were programmed with pSPUTK-CRD-BP DNA. The CRD-BP sequences in this DNA lack the upstream in-frame AUG and translation begins with the AUG noted in Figure 1. By immunoblotting, pSPUTK-CRD-BP generated an ~68 kDa protein that migrated at or close to authentic human and mouse CRD-BP (Fig. 3, lanes 1–3). An immunoreactive band was not observed in extract programmed with pSPUTK vector (Fig. 3, lane 4) or luciferase cDNA (data not shown). Therefore, the antibody detected CRD-BP and not an endogenous reticulocyte protein and the cDNA encodes CRD-BP. The cross-reacting band (p85) in the K562 and NIH 3T3 lanes is a protein observed previously (32). It is not related functionally to CRD-BP (see below).

Gel retardation assays were performed to determine if *in vitro* translated CRD-BP binds specifically to c-*myc* CRD RNA. RSW from K562 cell polysomes or from reticulocyte polysomes was incubated with c-*myc* CRD [^{32}P]RNA. RNA/protein complexes were visualized following non-denaturing gel electrophoresis. A complex was observed with RSW from K562 cells and from reticulocyte extract programmed with CRD-BP cDNA (Fig. 4A, lanes 1 and 2, respectively). These complexes migrated to similar or identical positions. An RNA/protein complex was not observed with RSW from luciferase (Luc), vector or no mRNA (None) control reactions (Fig. 4A, lanes 3–5). Therefore, *in vitro* translated CRD-BP, like its cell-derived counterpart, associates with c-*myc* CRD RNA *in vitro*.

Previous work had shown that cell-derived CRD-BP did not bind to other RNAs we tested, suggesting considerable specificity

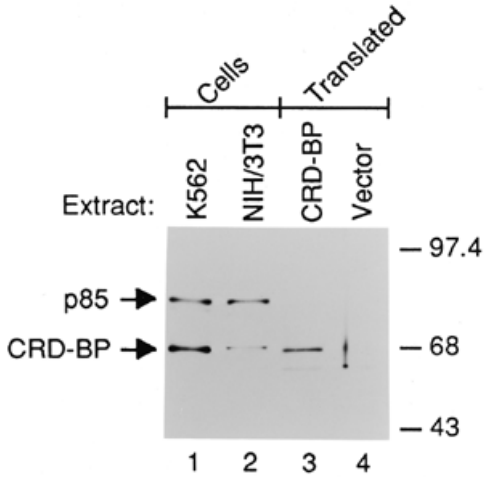

Figure 3. Immunoblotting assay showing co-migration of recombinant and cell-derived CRD-BP. RSW was prepared from polysomes from K562 or NIH 3T3 cells and from reticulocyte transcription/translation reactions programmed with CRD-BP DNA or with vector DNA. Approximately 7.5 × 10^5 cell equivalents of K562 or NIH 3T3 RSW or 3% of the RSW from a 50 µl translation reaction were electrophoresed and immunoblotted. Immunoreactive proteins were visualized using Supersignal chemiluminescent reagents (Pierce). The locations of the CRD-BP and a cross-reacting protein (p85) are indicated on the left. Prestained molecular mass markers are shown on the right in kDa.

for c-*myc* CRD RNA (30,31). A competition assay was performed to determine if *in vitro* translated CRD-BP exhibited similar specificity. Reactions contained c-*myc* CRD [^{32}P]RNA, CRD-BP and various unlabeled competitor RNAs at a 200-fold molar excess. Complex formation with CRD-BP was competed by c-*myc* CRD RNA but not by β-globin RNA (Fig. 4B, lanes 4–6), confirming that the cDNA encodes functional c-*myc* CRD-BP.

In view of the similarity between mouse CRD-BP and chicken ZBP1 (Table 1), we asked whether excess unlabeled, full-length β-actin zipcode RNA would block complex formation between recombinant CRD-BP and c-*myc* CRD [^{32}P]RNA. As expected, unlabeled c-*myc* CRD RNA did compete but globin RNA did not compete (Fig. 5, lanes 1–6). Unlabeled zipcode RNA containing the full-length 54 nt β-actin zipcode competed more than globin RNA but considerably less than c-*myc* CRD RNA (Fig. 5, lanes 7 and 8). Moreover, a 27 nt proximal zipcode [^{32}P]RNA probe that was used to purify ZBP1 (33) did not gel shift with recombinant mouse CRD-BP (data not shown). Therefore, although mouse

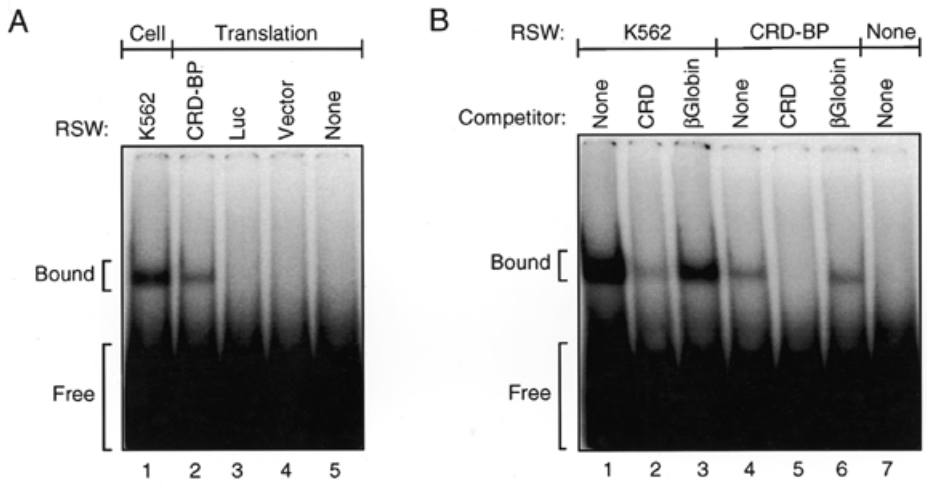

Figure 4. Gel retardation assay showing binding of recombinant CRD-BP to c-*myc* CRD RNA. (**A**) Gel retardation assay. RSW was prepared from K562 cell polysomes and from reticulocyte transcription/translation reactions programmed with mCRD-BP cDNA, luciferase cDNA (Luc) or vector DNA. Equivalent volumes (2 µl) of each RSW were incubated with 50 000 c.p.m. of c-*myc* CRD [^{32}P]RNA. None indicates no added protein. The positions of mCRD-BP/CRD complexes (Bound) and unbound RNA (Free) are indicated on the left. (**B**) Competition gel retardation assay. The indicated RSW was incubated with c-*myc* CRD [^{32}P]RNA in the presence or absence of buffer (None) or a 200-fold molar excess of unlabeled c-*myc* CRD RNA or β-globin RNA.

CRD-BP and chicken ZBP1 are similar, they might have somewhat different RNA-binding specificities.

Characterization of the binding region for CRD-BP in c-*myc* CRD RNA

[^{32}P]RNA probes from parts of the coding region and 3′-UTR of c-*myc* mRNA were analyzed by gel shifts to map the major binding site for the CRD-BP. As expected, avid binding was observed with nt 1705–1886 of c-*myc* mRNA (Fig. 6). Binding was also observed with a 1705–1792 probe, which is consistent with footprinting data showing that 1705–1792 is the core binding region (data not shown). All other probes bound less avidly or not at all.

Localization of CRD-BP to the cytoplasm and co-fractionation of CRD-BP with polyribosomes

Consistent with its role as a putative mRNA-binding protein, much of the CRD-BP in cytoplasmic lysates fractionates with polysomes (31). However, the CRD-BP, like FMRP and ZBP1 (33,45), contains nuclear localization and nuclear export signals (Fig. 1). To assess whether any CRD-BP co-fractionated with nuclei or with other subcellular fractions, exponentially growing K562 cells were lysed and separated into six fractions. Equal cell equivalents of each fraction were analyzed by immunoblotting. At least 95% of the total cell CRD-BP was in polysomes and >90% of this CRD-BP was eluted in the 1 M salt wash (Fig. 7A, RSW). Little or no CRD-BP was detected in post-polysomal supernatant (S130) or in nuclei (Fig. 7A). This result cannot be explained by indiscriminate proteolysis during sample preparation, because intact HSP90 was detected in all fractions (Fig. 7B). We conclude that, at steady-state, most of the CRD-BP is cytoplasmic and polysomal. In contrast, the cross-reacting p85 is predominantly nuclear (Fig. 7A).

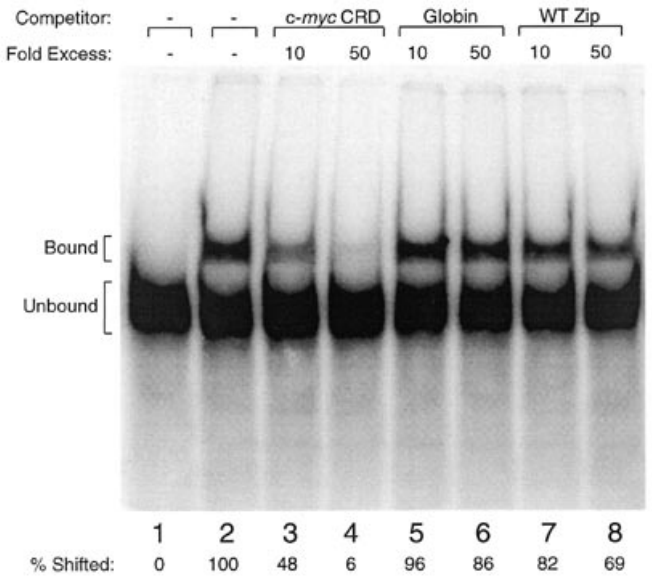

Figure 5. Gel retardation competition assays with c-*myc* CRD RNA β-globin RNA or β-actin zipcode RNA. Recombinant, His_6-tagged mCRD-BP was purified and 0.2 µg was incubated with c-*myc* CRD [^{32}P]RNA (20 fmol) with or without the indicated molar excess of unlabeled competitor RNAs. WT Zip refers to the 54 nt chicken β-actin zipcode sequence that is required for localizing β-actin mRNA in fibroblasts (33). Gel retardation was performed as per Figure 4. Bound indicates RNA/mCRD-BP complexes. The relative percentages of protein/RNA complex formation are noted at the bottom.

To confirm the cytoplasmic localization of the CRD-BP, we used immunofluorescence to localize transiently expressed, FLAG-tagged CRD-BP. H4IIE and 293 cells expressing FLAG–CRD-BP exhibited strong staining that was predominantly cytoplasmic (Fig. 8). Little or no FLAG–CRD-BP was detected within nuclei. Neither untransfected cells nor cells transfected

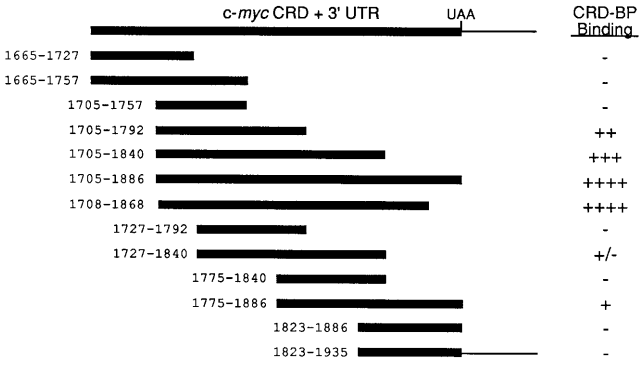

Figure 6. Mapping the binding site of CRD-BP on c-*myc* CRD RNA. Portions of the c-*myc* mRNA coding region and 3′-UTR were amplified by PCR with the 5′ primer including an SP6 promoter. [^{32}P]RNA was prepared from each template and analyzed by gel retardation for CRD-BP binding. (++++), (+++), (++) and (+) indicate 100, ~70, ~40 and ~10% binding. (+/–) indicates that a weak protein/RNA complex was visualized after prolonged exposure of the blot to the PhosphorImager screen.

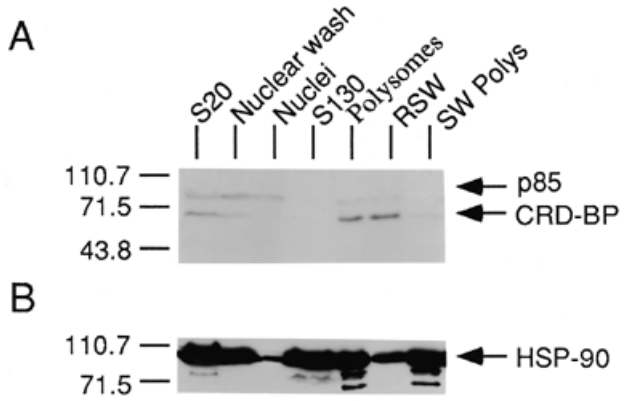

Figure 7. Co-fractionation of endogenous CRD-BP with K562 cell polysomes and absence of CRD-BP in nuclei. Subcellular fractions were prepared from exponentially growing K562 cells. Equal cell equivalents (6×10^5) of each fraction were immunoblotted and the membrane was probed with (**A**) anti-CRD-BP IgY or (**B**) anti-HSP90 IgG. The positions of molecular mass markers are indicated in kDa on the left.

with untagged CRD-BP were stained with the anti-FLAG antibody and no cells were stained when incubated only with the FITC-conjugated anti-mouse IgG secondary antibody (data not shown).

We have suggested that some of the polysome-associated CRD-BP in the cell is bound to c-*myc* mRNA (30). To investigate whether some of it might also co-fractionate with ribosomal subunits, polysomes were dissociated into subunits plus mRNP by EDTA treatment and fractionated in a sucrose gradient. Small and large ribosomal subunits sedimented primarily in fractions 6–11 and 10–14, respectively (Fig. 9A and B). CRD-BP was detected over a large portion of the gradient and appeared to co-sediment with both large and small subunits (Fig. 9C). This pattern is similar to that of another putative mRNA-binding protein, FMRP (34,43–45). Some CRD-BP also pelleted to the bottom of the gradient. This material probably contains undissociated polysomes and monosomes. In summary, the CRD-BP co-sediments with ribosomal subunits, although the data do not address whether the CRD-BP is actually associated with the subunits. p85 was found at and near the top of the gradient and did not co-sediment with subunits (Fig. 9C), confirming that the CRD-BP and p85 are immunologically related but are functionally distinct.

DISCUSSION

Properties of recombinant CRD-BP

We have described the cloning and further characterization of the CRD-BP, a protein that binds *in vitro* to the CRD of c-*myc* mRNA. In cells, the c-*myc* CRD is a mRNA-destabilizing element whose function is somehow connected to translation (18–22). *In vitro*, the CRD binds to the CRD-BP and appears to shield c-*myc* mRNA from an endoribonuclease (22,30,31). Recombinant CRD-BP, like authentic CRD-BP from cells, migrates in gels at ~68 kDa (Fig. 3), binds with considerable specificity to CRD RNA (Figs 4 and 5) and remains bound to the RNA at physiological salt in high concentrations of heparin (Fig. 4).

Comparison of the CRD-BP with related proteins

The CRD-BP is homologous to ZBP1, hKOC, xTFB3 and Vg1 RBP/Vera (Table 1), all of which appear to represent a unique subfamily of RNA-binding proteins with two RRMs, an RGG box and four KH domains. Other putative RNA-binding proteins also contain four KH domains (51), but these domains are neither organized nor spaced in the same way as in the CRD-BP family. The CRD-BP also contains one putative nuclear localization sequence and two putative nuclear export sequences (Fig. 1). We do not know if the CRD-BP actually shuttles between the nucleus and the cytoplasm, as do some other RNA-binding proteins (52). If it does shuttle, however, it appears to spend most of its time in the cytoplasm (below).

Various functions have been ascribed to members of this protein family, each of which was identified based on different features and nucleic acid-binding specificities. For example, ZBP1 was identified based on its affinity for a 27 nt RNA containing the proximal half-site of the 54 nt β-actin mRNA zipcode, an mRNA-localizing signal (33). Aside from stretches of A/C-richness, the RNA-binding sites in c-*myc* and β-actin mRNAs have no obvious similarities and a gel shift competition experiment indicates that the CRD-BP does not bind avidly to the 54 nt zipcode RNA (Fig. 5). Perhaps each family member has a unique function in various cytoplasmic and nuclear compartments. The CRD-BP is thought to protect the c-*myc* mRNA coding region from an endoribonuclease (30). In this respect, it is similar to the iron response protein (IRP), which is thought to protect the 3′-UTR of transferrin receptor mRNA from RNase attack (reviewed in 53).

CRD-BP in the cytoplasm

It was essential for us to determine where the CRD-BP is within the cell, because the CRD-BP sequence includes nuclear localization and export motifs (Fig. 1). We find that CRD-BP is cytoplasmic and co-fractionates with polysomes and ribosomal subunits (Figs 7–9). We do not know if the CRD-BP is actually associated with the subunits or merely co-sediments with them.

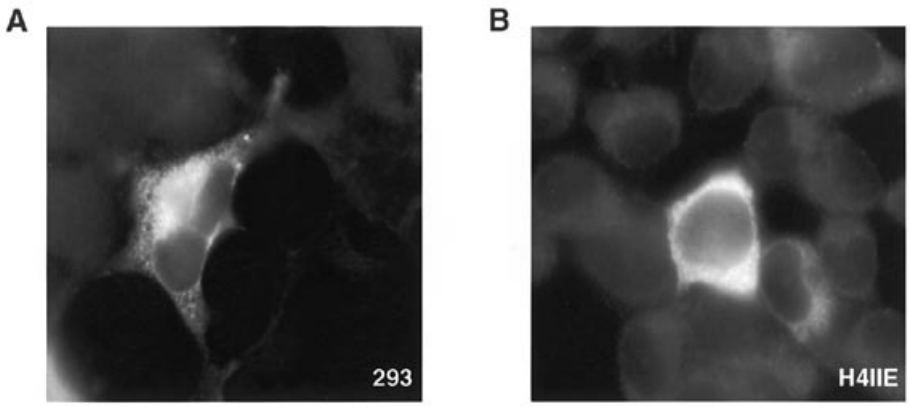

Figure 8. Immunofluorescent localization of FLAG-tagged CRD-BP in the cytoplasm of 293 and H4IIE cells. FLAG-tagged CRD-BP was transiently expressed in 293 (**A**) or H4IIE (**B**) cells. Cells were then stained and visualized via indirect immunofluorescence microscopy (Materials and Methods).

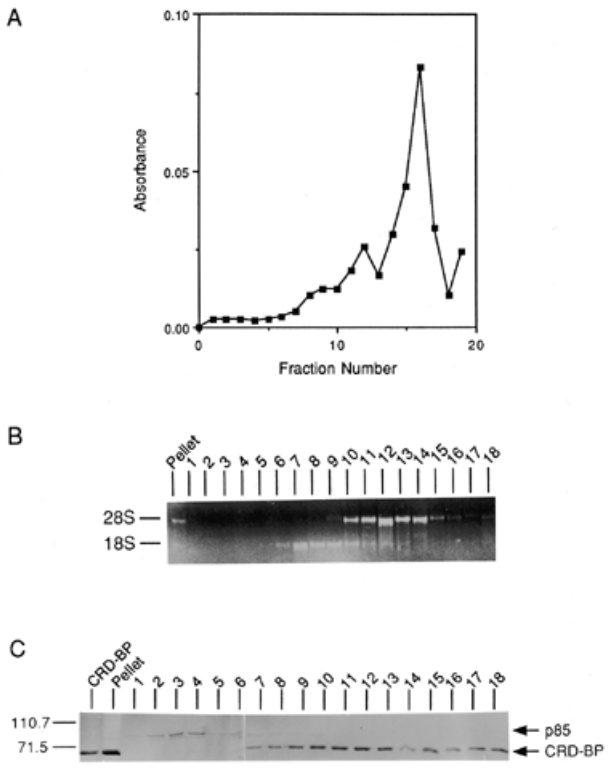

Figure 9. Co-sedimentation of the CRD-BP with ribosomal subunits. EDTA-dissociated K562 cell ribosomal subunits and mRNP were fractionated in a linear 5–30% sucrose gradient containing EDTA. Fraction 1 is the top of the gradient, fraction 18 is the last gradient fraction and fraction 19 is material resuspended from the bottom of the centrifuge tube. (**A**) Absorbance at 260 nm. (**B**) RNA from an aliquot of each fraction electrophoresed in a 1% agarose gel and visualized with ethidium bromide. The 28S and 18S rRNAs are noted on the left. (**C**) An aliquot of each fraction analyzed by immunoblotting using anti-CRD-BP IgY. Molecular mass markers are indicated in kDa on the left. CRD-BP and the cross-reacting p85 are noted on the right.

In either case, these findings are important for two reasons: (i) they show that the CRD-BP spends little time, if any, in the nucleus; (ii) they suggest that the CRD-BP might bind not only to mRNAs but also to ribosomes. Consistent with this possibility, xTFB3 protein in frog eggs is localized in the 'heavy ooplasmic fraction', which is enriched in ribosomes (48,54). Perhaps ribosome-bound CRD-BP molecules constitute a reservoir of protein that is recruited when needed to bind to mRNAs such as c-*myc*. In these respects, the CRD-BP is similar to FMRP (34,43–45). Both proteins co-sediment with ribosomes/polysomes (Fig. 9; 34,43–45) and FLAG–CRD-BP exhibits a punctate, cytoplasmic immunofluorescence staining pattern similar to that of FLAG–FMRP (Fig. 8; 34,53,55). We find no evidence for CRD-BP localization to a single region of the cytoplasm.

CRD-BP as an oncofetal protein

The c-*myc* CRD-BP is developmentally regulated, being expressed abundantly in fetal and neonatal life but not in adults (32). It is unknown whether xTFB3 is expressed in adults, but it is certainly expressed during early *Xenopus* development (48). Apparently, the CRD-BP is not required for cell viability, since perfectly normal adult animals do not express the CRD-BP at levels detectable by immunoblotting and/or gel retardation assays (32). Perhaps it has a special role in embryonic/fetal development.

The CRD-BP is also expressed in many cell lines, all of which are neoplastic or pre-neoplastic (Figs 3 and 4 and data not shown) and it is similar to the hKOC protein, which is overexpressed in human cancers (Fig. 2 and Table 1; 47). These findings suggest that the CRD-BP might be an oncofetal protein. If so, it would join a growing list of RNA-binding proteins that influence early development and/or carcinogenesis (56–60). In view of these potential links between the CRD-BP, early development and neoplasia, it should be interesting to learn if the CRD-BP is induced in tumor tissues of adult organisms and whether its over- or underexpression affects embryonic/fetal development.

ACKNOWLEDGEMENTS

We thank Dr Alan Poland for anti-HSP90 antibody, Yuri Oleynikov and Rob Singer for the DNA template for preparing the 54 nt chicken β-actin zipcode RNA and Linda Robinson and Rich Stewart for thoughtful comments on the manuscript. The GenBank accession no. for mouse CRD-BP cDNA is AF061569. This work was supported by Public Health Service grants CA63676, CA23076 and CA09230. P.L. was the recipient of an American Cancer Society post-doctoral grant (PF-3870).

REFERENCES

1 Ayer,D.E. and Eisenman,R.N. (1993) *Genes Dev.*, **7**, 2110–2119.
2 Ayer,D.E., Kretzner,L. and Eisenman,R.N. (1993) *Cell*, **72**, 211–222.
3 Zervos,A.S., Gyuris,J. and Brent,R. (1993) *Cell*, **72**, 223–232.
4 Spencer,C.A. and Groudine,M. (1991) *Adv. Cancer Res.*, **56**, 1–48.
5 Coppola,J.A. and Cole,M.D. (1986) *Nature*, **320**, 760–763.
6 Freytag,S.O., Dang,C.V. and Lee,W.M.F. (1990) *Cell Growth Differentiat.*, **1**, 339–343.
7 Evan,G.I., Wyllie,A.H., Gilbert,C.S., Littlewood,T.D., Land,H., Brooks,M., Waters,C.M., Penn,L.Z. and Hancock,D.C. (1992) *Cell*, **69**, 119–128.
8 Adams,J.M., Harris,A.W., Pinkert,C.A., Corcoran,L.M., Alexander,W.S., Cory,S., Palmiter,R.D. and Brinster,R.L. (1985) *Nature*, **318**, 533–538.
9 Klein,G. (1989) *Genes Chromosomes Cancer*, **1**, 3–8.
10 Lüscher,B. and Eisenman,R.N. (1990) *Genes Dev.*, **4**, 2025–2035.
11 Spotts,G.D. and Hann,S.R. (1990) *Mol. Cell. Biol.*, **10**, 3952–3964.
12 Lutterbach,B. and Hann,S.R. (1994) *Mol. Cell. Biol.*, **14**, 5510–5522.
13 Morello,D., Asselin,C., Lavenu,A., Marcu,K.B. and Babinet,C. (1989) *Oncogene*, **4**, 955–961.
14 Gruppuso,P.A., FitzGerald,M.J. and Fausto,N. (1993) *Pediat. Res.*, **33**, 49A.
15 Morello,D., Lavenu,A. and Babinet,C. (1990) *Oncogene*, **5**, 1511–1519.
16 Steer,C.J. (1996) *FASEB J.*, **10**, 559–573.
17 Jones,T.R. and Cole,M.D. (1987) *Mol. Cell. Biol.*, **7**, 4513–4521.
18 Wisdom,R. and Lee,W. (1990) *J. Biol. Chem.*, **265**, 19015–19021.
19 Wisdom,R. and Lee,W. (1991) *Genes Dev.*, **5**, 232–243.
20 Yeilding,N.M., Rehman,M.T. and Lee,W.M.F. (1996) *Mol. Cell. Biol.*, **16**, 3511–3522.
21 Yeilding,N.M. and Lee,W.M.F. (1997) *Mol. Cell. Biol.*, **17**, 2698–2707.
22 Herrick,D.J. and Ross,J. (1994) *Mol. Cell. Biol.*, **14**, 2119–2128.
23 Lavenu,A., Pistoi,S., Pournin,S., Babinet,C. and Morello,D. (1995) *Mol. Cell. Biol.*, **15**, 4410–4419.
24 Morello,D., Lavenu,A., Pournin,S. and Babinet,C. (1993) *Oncogene*, **8**, 1921–1929.
25 Pistoi,S., Roland,J., Babinet,C. and Morello,D. (1996) *Mol. Cell. Biol.*, **16**, 5107–5116.
26 Ross,J. and Kobs,G. (1986) *J. Mol. Biol.*, **188**, 579–593.
27 Ross,J., Peltz,S.W., Kobs,G. and Brewer,G. (1986) *Mol. Cell. Biol.*, **6**, 4362–4371.
28 Peltz,S.W. and Ross,J. (1987) *Mol. Cell. Biol.*, **7**, 4345–4356.
29 Brewer,G. and Ross,J. (1988) *Mol. Cell. Biol.*, **8**, 1697–1708.
30 Bernstein,P.L., Herrick,D.J., Prokipcak,R.D. and Ross,J. (1992) *Genes Dev.*, **6**, 642–654.
31 Prokipcak,R.D., Herrick,D.J. and Ross,J. (1994) *J. Biol. Chem.*, **269**, 9261–9269.
32 Leeds,P., Kren,B.T., Boylan,J.M., Betz,N.A., Steer,C.J., Gruppuso,P.A. and Ross,J. (1997) *Oncogene*, **14**, 1279–1286.
33 Ross,A.F., Oleynikov,Y., Kislauskis,E.H., Taneja,K.L. and Singer,R.H. (1997) *Mol. Cell. Biol.*, **17**, 2158–2165.
34 Siomi,M.C., Zhang,Y., Siomi,H. and Dreyfuss,G. (1996) *Mol. Cell. Biol.*, **16**, 3825–3832.
35 Harlowe,E. and Lane,D. (1988) *Antibodies: A Laboratory Manual*. Cold Spring Harbor Laboratory Press, Cold Spring Harbor, NY, pp. 359–420.
36 Kozak,M. (1989) *J. Cell. Biol.*, **108**, 229–241.
37 Kenan,D.J., Query,C.C. and Keene,J.D. (1991) *Trends Biochem. Sci.*, **25**, 214–220.
38 Burd,C.G. and Dreyfuss,G. (1994) *Science*, **265**, 615–621.
39 Gil,A., Sharp,P.A., Jamison,S.F. and Garcia-Blanco,M.A. (1991) *Genes Dev.*, **5**, 1224–1236.
40 Piñol-Roma,S., Swanson,M.S, Gall,J.G. and Dreyfuss,G. (1989) *J. Cell Biol.*, **109**, 2575–2587.
41 Jansen,R.P., Hurt,E.C., Kern,H., Lehtonen,H., Carmo-Fonseca,M., Lapeyre,B. and Tollervey,D. (1991) *J. Cell Biol.*, **113**, 715–729.
42 Srivastava,M., McBride,O.W., Fleming,P.J., Pollard,H.B. and Burns,A.L. (1990) *J. Biol. Chem.*, **265**, 14922–14931.
43 Ashley,C.T., Wilkinson,K.D., Reines,D. and Warren,S.T. (1993) *Science*, **262**, 563–565.
44 Siomi,H., Siomi,M.C., Nussbaum,R.L. and Dreyfuss,G. (1993) *Cell*, **74**, 291–298.
45 Eberhart,D.E., Malter,H.E., Feng,Y. and Warren,S.T. (1996) *Hum. Mol. Genet.*, **5**, 1083–1091.
46 Ciccarelli,R.B., Gunyuzlu,P., Huang,J., Scott,C. and Oakes,F.T. (1991) *Nucleic Acids Res.*, **19**, 6007–6113.
47 Müeller-Pillasch,F., Lacher,U., Wallrapp,C., Micha,A., Zimmerhackl,F., Hameister,H., Varga,G., Friess,H., Büchler,M., Beger,H.G., Vila,M.R., Adler,G. and Gress,T.M. (1997) *Oncogene*, **14**, 2729–2733.
48 Pfaff,S.L. and Taylor,W.L. (1992) *Dev. Biol.*, **151**, 306–316.
49 Havin,L., Git,A., Elisha,Z., Oberman,F., Yaniv,K., Scwartz,S.P., Standart,N. and Yisraeli,J.K. (1998) *Genes Dev.*, **12**, 1593–1598.
50 Deshler,J.O., Highett,M.I., Abramson,T. and Schnapp,B.J. (1998) *Curr. Biol.*, **8**, 489–496.
51 Musco,G., Stier,G., Joseph,H., Antonietta,M., Morelli,C., Nilges,M., Gibson,T.J. and Pastore,A. (1996) *Cell*, **85**, 237–245.
52 Piñol-Roma,S. and Dreyfuss,G. (1992) *Nature*, **355**, 730–732.
53 Harford,J.B., Rouault,T.A. and Klausner,R.D. (1994) In Brock,J.H., Halliday,J.W., Pippard,M.J. and Powell,L.W. (eds) *Iron Metabolism in Health and Disease*. W.B.Saunders, Philadelphia, PA, pp. 123–149.
54 Lohka,M.J. and Masui,Y. (1984) *J. Cell Biol.*, **98**, 1222–1230.
55 Feng,Y., Absher,D., Eberhart,D.E., Brown,V., Malter,H.E. and Warren,S.T. (1997) *Mol. Cell*, **1**, 109–118.
56 Bandziulis,R.J., Swanson,M.S. and Dreyfuss,G. (1989) *Genes Dev.*, **3**, 431–437.
57 Herschlag,D. (1995) *J. Biol. Chem.*, **270**, 20871–20874.
58 Shamoo,Y., Abdul-Manan,N. and Williams,K.R. (1995) *Nucleic Acids Res.*, **23**, 725–728.
59 Gao,F.-B. and Keene,J.D. (1996) *J. Cell Sci.*, **109**, 579–589.
60 Cooke,H.J. and Elliott,D.J. (1997) *Trends Genet.*, **13**, 87–89.